e-ISSN 1734-9168
http://www.isez.pan.krakow.pl/en/folia-biologica.html

Folia Biologica (Kraków), vol. 71 (2023), No 4
https://doi.org/10.3409/fb_71-4.20

Spermatogenesis and spermatozoon ultrastructure in the jawed bloodfeeding land leech *Haemadipsa japonica* (Hirudinida: Hirudiniformes) from Japan

Raja Ben Ahmed, Takafumi Nakano, Joanna Piątek, Robert Krzyzczyk, and Piotr Świątek

Accepted December 12, 2023 *Published online December 29, 2023* *Issue online December 29, 2023*

Original article

Ben Ahmed R., Nakano T., Piątek J., Krzyzczyk R., Świątek P. 2023. Spermatogenesis and spermatozoon ultrastructure in the jawed bloodfeeding land leech *Haemadipsa japonica* (Hirudinida: Hirudiniformes) from Japan Folia Biologica (Kraków) **71**: 207-220.

The aim of this study is to describe spermatogenesis and spermiogenesis in the jawed sanguivorous land leech *Haemadipsa japonica* Whitman, 1886, for the first time, using both light and electron microscopy. Spermatogenesis occurs within testisacs, where numerous cysts (clusters) of interconnected spermatogonia, spermatocytes and spermatids freely float in the fluid. In a given cyst, the interconnected germ cells develop in synchrony, i.e. spermatogonial cysts, and cysts with spermatocytes or spermatids can be observed. During spermiogenesis, the spermatids transform into typical hirudinid filiform mature spermatozoa. The ultrastructure of *H. japonica* spermatozoa is broadly similar to that already described for *Haemadipsa zeylanica*. The sperm has an anterior and a posterior acrosome, an elongated nucleus with two different morphological regions (an apical corkscrew-shaped region and a basal twisted column-shaped region), a single straight mitochondrion (midpiece) enclosed by a sheath of electron-dense material, and a flagellum with a prominent central sheath arrangement followed by a tapering appendage. A comparison with the previously described spermatozoa from other Clitellata species reveals that the greatest resemblance is to Hirudiniformes.

Key words: testis, germline cysts, spermiogenesis, Annelida, phylogeny.

Raja Ben Ahmed✉, Faculté des Sciences de Tunis, Ecologie, Biologie et Physiologie des organismes aquatiques (LR18ES41), Université de Tunis El Manar, Tunis, Tunisia.
E-mail: raja_benahmed@yahoo.fr
Takafumi Nakano, Department of Zoology, Graduate School of Science, Kyoto University, Kyoto 606-8502, Japan.
Joanna Piątek, Robert Krzyzczyk, Piotr Świątek, Institute of Biology, Biotechnology and Environmental Protection, Faculty of Natural Sciences, University of Silesia in Katowice, Poland.

Land leeches are terrestrial jawed hematophagous leeches, known from subtropical and tropical regions around the Indian and Pacific Oceans (Lai *et al.* 2011). About 60 described land leech species are recognised, of which 50 belong to the family Haemadipsidae; while the rest are in the family Xerobdellidae (Sket & Trontelj 2008). Despite recent papers devoted to land leeches, their taxonomic identification at a species level, diversity and ecology remain poorly understood (Lai *et al.* 2011). Haemadipsid leeches are a source of invertebrate-derived ingested DNA (iDNA), which can be used to monitor animal biodiversity (Lai *et al.* 2011; Schnell *et al.* 2015; Tessler *et al.* 2018; Hanya *et al.* 2019; Fahmy *et al.* 2019). Nevertheless, the histological and ultrastructural details of the land leeches' reproductive systems and gametogenesis are largely unknown (Ben Ahmed *et al.* 2015a), although they may present some interesting phylogenetic features. In fact, numerous ultrastructural details of the sperm ultrastructure have been used to analyse the phylogeny of certain Clitellata taxa, including leeches (e.g. Ferra-

guti & Erséus 1999; Jamieson 2006; Marotta *et al.* 2008; Marotta & Ferraguti 2009). These studies have revealed that the sperm ultrastructure carries useful phylogenetic information that may be crucial in understanding relationships within the phylum and establishing a taxonomic system (Jamieson 2006; Marotta & Ferraguti 2009; Marotta *et al.* 2008). Recently, knowledge about the male gametogenesis of true leeches (Hirudinida) has increased significantly. There are numerous papers in this field; however, most of the available ultrastructural studies have only focused on spermatid development and the morphology of the mature sperm (Arcidiacono 1979; Garavaglia *et al.* 1974; Gouda 2013; Malécha 1975; Ben Ahmed *et al.* 2015b). In contrast, reports presenting the whole process of spermatogenesis (from spermatogonia to mature sperm) are limited (Gouda 2013; Ben Ahmed *et al.* 2015a; Ben Ahmed *et al.* 2019). Furthermore, although there are ultrastructural studies devoted to the spermatogenesis of several freshwater leeches (Bonet & Molinas 1988; Bonet *et al.* 1988; Gouda 2013; Ben Ahmed *et al.* 2015a,b; Ben Ahmed *et al.* 2019), only one study restricted to the description of the mature spermatozoa of the terrestrial leech *Haemadipsa zeylanica* is available (for details, see Ben Ahmed *et al.* 2015b). This latter study gives only a rough idea about the sperm ultrastructure and contains no information about spermatogenesis and spermiogenesis. Accordingly, additional research on land leeches is necessary to fill this gap and to find evidence of the spermatozoa species specificity, as well as to identify conservative traits and to show the possibility or the impossibility of using sperm morphology as an additional morphological trait for phylogeny. *Haemadipsa japonica* Witman (Haemadipisade) is a leech endemic to East Asia that feeds on different animal hosts, mainly on sika deer (*Cervus nippon*) (Morishima *et al.* 2022). Its blood-feeding behaviour and its use in traditional medicine have made the leech a subject of interest (Lai *et al.* 2011). Recently, *H. japonica* was the subject of studies devoted to its host biodiversity based on iDNA analyses (Hanya *et al.* 2019; Morishima *et al.* 2022). The goals of this study were: (1) to describe for the first time the process of spermatogenesis at the light and electron microscopy level in *Haemadipsa japonica*, as well as the sperm maturation and ultrastructure; (2) to provide further characteristics that may elucidate the phylogenetic position of the family; and (3) to obtain a safe basis for discussions on spermatogenesis and the sperm ultrastructure of land leeches.

Material and Methods

Specimen collection

Specimens of *Haemadipsa japonica* Whitman, 1886, were collected from five localities in Japan during 2011-2018 (Table 1). In total, 20 specimens were used in this study.

Light (LM) and electron microscopy (TEM)

The leeches were fixed and processed as described previously (Urbisz *et al.* 2020). Briefly, before the initial fixation with 2.5% glutaraldehyde in a 0.1 M phosphate buffer (pH 7.4), the leeches were narcotised with sparking mineral water. After dissection, the testisacs were fixed in 2.5% glutaraldehyde in the same buffer at room temperature for several days. Then, the testisacs were washed in a phosphate buffer and postfixed for 1 h in 1% OsO_4 in the same buffer, and dehydrated in a graded series of ethanol replaced with acetone, before being embedded using an Epoxy Embedding Medium Kit (Sigma, St. Louis, MO, USA). Semi-thin sections (0.7-µm thick) were cut on an RMC Power XT ultramicrotome (RMC Boeckeler, Tucson, AZ) and stained with 1% methylene blue in a 1% sodium biborate solution at room temperature for 30 s. The sections were examined under an Olympus BX60 microscope, equipped with an XC50 digital camera (Olympus) and cellSens Standard software (Olympus). Ultra-thin sections

Table 1

Specimen information, collection localities and exact coordinates

Taxon	Locality	Collection data	Coordinates
Haemadipsa japonica	Takidanitoge Pass, Kyoto, Honshu Island	1 November 2011	(35°08′ N, 135°45′ E)
	the University of Tokyo Chiba Forest, Chiba, Honshu Island	11 June 2012	(35°08.4′ N, 140°09.1′ E)
	Nibetsu, Akita, Honshu Island	3 September 2014	(39°47′ 48.6″N, 140°14′ 06.6″E)
	Hakiai, Kumamoto, Kyushu Island	21 October 2017	(32°24′ 50.1″N, 130°51′ 51.5″E)
	Ko-notani, Nara, Honshu Island	4 August 2018	(34°15′ 34.8″N, 136°05′ 50.5″E)

(60 nm thick) were cut on a Leica UC7 ultramicrotome (Leica Microsystems, Wetzlar, Germany). The ultrathin sections were contrasted with uranyl acetate (30 min) and lead citrate (20 min), and were examined using a Hitachi H500 electron microscope at 75 kV.

Results

General morphology of the testis

The wall of the testis (33.3 μm thick) is composed of thin coelomic epithelia interconnected via connective tissue with a well-developed extracellular matrix and muscle fibres (Fig. 1A). The cells directly contacting the testis lumen are ciliated (Fig. 1A *inset*.) The testes of the studied species are filled with hundreds of syncytial germline cysts (clones, clusters and morulae; for more details about the terminology, see Ben Ahmed *et al.* 2019). Each cyst is formed by dozens of germ cells in the same stage of development (Fig. 1A). In a given cyst, each germline cell is connected by one intercellular (cytoplasmic) bridge to the mass of central, anuclear cytoplasm (Fig. 1B). This central cytoplasm is termed the 'cytophore'. The spermatogonia have large, oval nuclei that occupy most of the cell volume (Fig. 1B). Within the nuclei, prominent, dark-staining nucleoli occur (Fig. 1B). When meiosis begins, the primary spermatocytes become rounded and are noticeably smaller than the spermatogonia (Fig. 1F). They have a spherical, centrally located nuclei (Fig. 1F). The early spermatids show the presence of two structures that take on a deeper stain, situated at the apical and basal pole of the cell, respectively (Fig. 1D). The mid-spermatids acquire a longitudinal axis and a polarity, with the rudiments of a flagellum becoming apparent at their distal end (Fig. 1D). The spermatids remain interconnected via intercellular bridges and the cytophore (Figs 1C, D). At this stage of sperm differentiation, the cytophore increases its volume due to the progressive accumulation of residual cytoplasm with organelles (Figs 1 C, D). Late spermatids can be recognised by their nuclei, which undergo nuclear condensation, become elliptical and then elongate (Fig. 1 C). They remain attached to the cytophore, with their flagella facing toward the testisacs' lumen (Fig. 1 G). At this step, degeneration inside the cytophore was observed (Fig. 1G). The spermatozoa detach from the cytophore and leave the testes *via* the vas deferens, and then enter the epididymis, where they form an accumulation (Fig. 1E). Semithin cross-sections through the epididymis show that it is filled with bundles of spermatozoa (Fig. 1E).

Ultrastructural characteristics of spermatogenic cells

Spermatogonia

the spermatogonia (4.3 μm ± 0.75 μm in diameter (n = 4)) are joined into cysts via intercellular bridges (Figs 1B. 2A, B). They are pear-shaped cells, with a large, irregularly shaped nucleus (3.1 μm ± 0.16μm in diameter (n = 4)) occupying almost the whole cell volume (Figs 1B. 2A, B). A nucleolus and dense patches of condensed heterochromatin can be seen throughout the nucleoplasm (Figs 2A, B). Lipid droplets and cytoplasmic organelles, such as free ribosomes and scattered mitochondria with a dense matrix, are also present (Figs 2A, B). The Golgi complex and numerous mitochondria are located at the basal cell pole (proximal to the intercellular bridge) (Fig. 2A). Spherical or elongated mitochondria form accumulations (Figs 2A, B).

Spermatocytes

This stage of sperm differentiation was not observed during the TEM analysis. The transition from spermatogonia to the first spermatocytes, and then to the second spermatocytes, can be a relatively rapid process, and these transitions may occur quickly compared to some of the other cellular processes.

Spermiogenesis

Early spermatids

The early spermatids (3.3 μm ± 0.152 in diameter (n = 5)) are polarised cells with an ovoid-shaped nucleus with dispatched chromatin (Figs 3A-C). The presence of a large mitochondrion characterises this stage. This latter structure has an electron-dense matrix and is closely adherent to the nucleus (Figs 3A-B). The mitochondrion engages the basal (future distal end of the spermatozoa) region of the cell (not shown). In the periphery of the nucleus, the chromatin begins forming a circle of condensed chromatin. At this stage, the first step of organelle redistribution was observed. The apical region (the pole opposite to the intercellular bridge) is now marked by a Golgi complex in close vicinity to the nucleus (Figs 3C, D). The acrosome tube of the 'proacrosome vesicle' (PAV) is positioned near the Golgi complex, which consists of a stack of flattened cisternae (Figs 3A, B). The intercellular bridges have the form of rings, made up of an electron-opaque material that connects the spermatids to the cytophore (Figs 3A-C). The distal centriole gives rise to the flagellum (Figs 3B, D). It begins to appear just beneath the cell membrane (Fig. 3 B). The flagellum is situated in the opposite cell pole than the cytoplasmic bridge, which connects the cell to the cytophore. The latter contains free ribosomes, mitochondria and ER (Figs 3A-C).

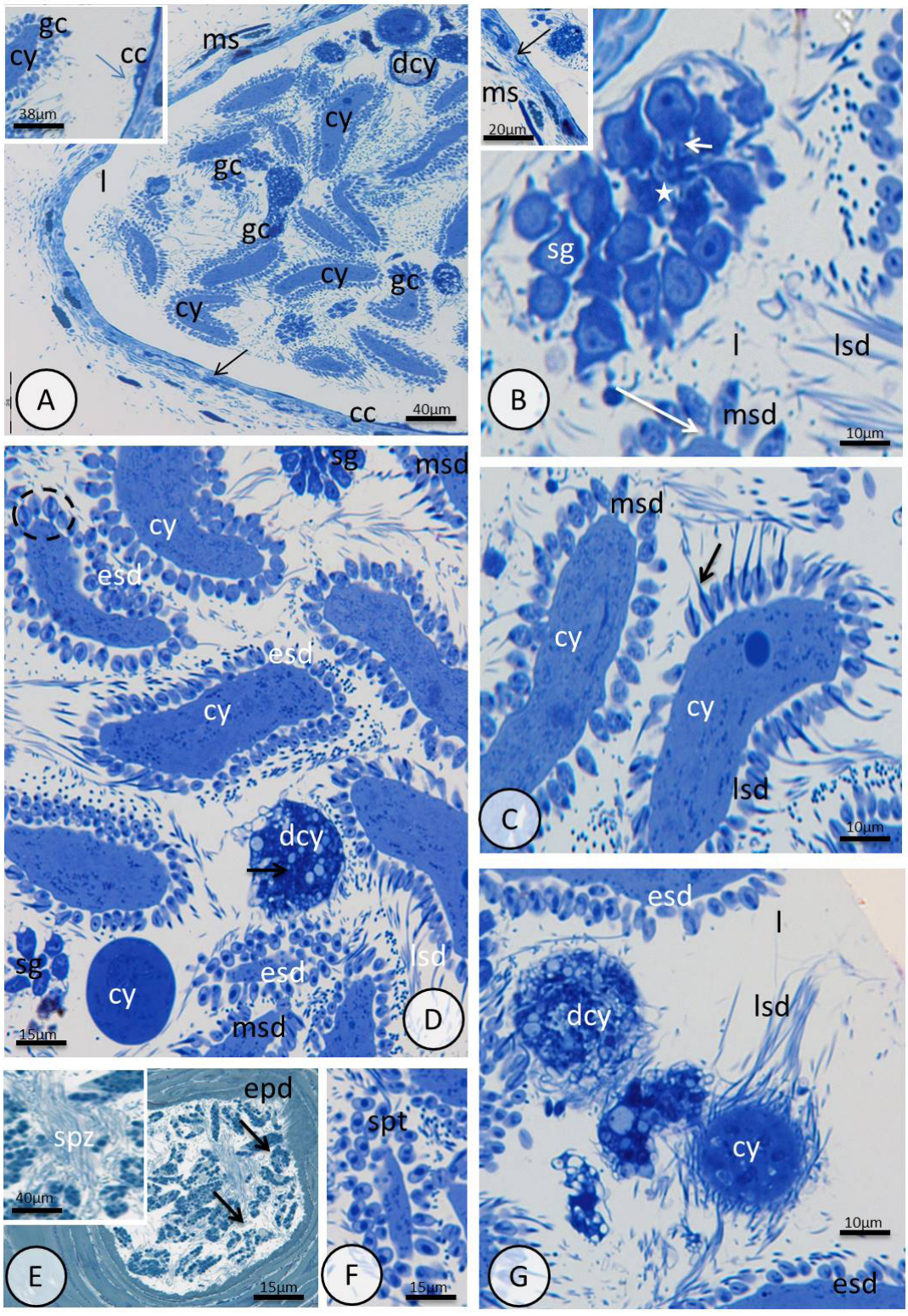

Fig. 1. Morphology of the testis. A – Germline cysts are visible inside the testis. Cysts are formed by germ cells (gc), connected to a common cytoplasmic mass, the cytophore (cy). Parietal ciliated cells (cc), muscle cells (ms), epithelium (black arrow), degenerative cytophore (dcy) and testis lumen (l) are also visible. *Inset:* Parietal ciliated cells and cyst fragments are visible. Note germ cells (gc) and cytophore (cy); arrow points to the cilia. B – Spermatogonial cyst. Spermatogonia (sg) are attached to the cytophore (star) by intercellular bridges (arrows), with fragments of cysts with mid-spermatids (msd) and late spermatids (lsd) visible. The long arrow marks the intercellular bridge. *Inset*: details of the testis wall. Muscle cells (ms), testis lumen (l) and epithelium (arrow) are visible. C – Two cysts in two developmental stages: clone with mid-spermatids (msd) and late spermatids (lsd). Cytophore (cy); arrow points to the flagellum. D and G – Germline cysts in different developmental stages: spermatogonia (sg); early spermatids (esd); mid-spermatids (msd); and late elongated spermatids (lsd). Late spermatids (lsd) are still attached to the cytophore (cy) (dashed line). Degenerating cytophores (dcy) are visible. E – Bundles of spermatozoa (arrows) inside the epididymis (epd). *Inset*: spermatozoa (spz). F – Spermatocytes (spt). Light microscopy (LM), Epon semithin sections, with methylene blue staining.

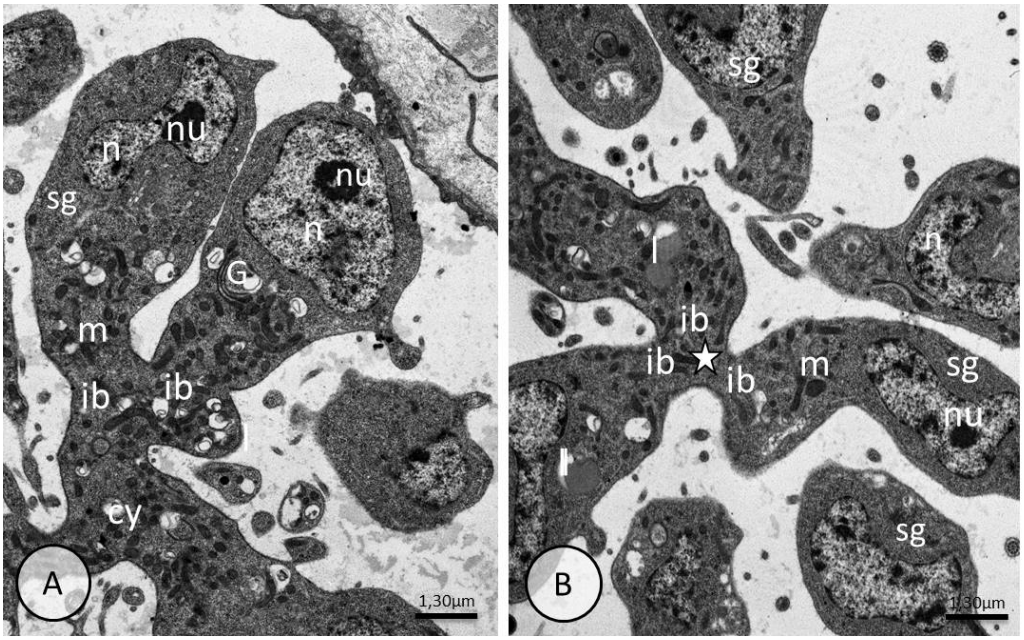

Fig. 2. Spermatogonial cysts. A-B – Spermatogonia (sg) are connected to the cytophore (cy) via intercellular bridges (ib). The cytoplasm of the spermatogonia is occupied by large nuclei (n) with nucleolus (nu), lipid (l), Golgi complex (G) and mitochondria aggregations (m). Numerous mitochondria are also present in the cytophore (asterisk). Transmission electron microscopy (TEM).

Mid-spermatids

In the next stage of sperm maturation, the final distribution of the organelles starts to be accomplished**.** The Golgi complex and the PAV are situated in the basal part of the cell, close to the bridge. In contrast, the mitochondrion occupies the pole which faces the intercellular bridge (the apical one) (Fig. 3D). At the same time, the chromatin continues to condense and starts to form electron-dense fibres (Fig. 3E). The nucleus is elliptical (Fig. E). Moreover, the flagellum continues to grow.

Late spermatids

The late spermatids and the cytophore remain interconnected by intercellular bridges (Figs 3F-J). They can be recognised by further cell elongation (Figs 3F, G, H, I, J). The acrosome takes its final position and shape; the chromatin becomes fibrillar and the diameter of the nucleus decreases. Likewise, the midpiece mitochondrion reaches its final arrangement throughout the axoneme.

Acrosome morphogenesis

The early stage of acrosome morphogenesis is marked by the appearance of a characteristic PAV near the Golgi complex (Fig. 4A). The fusion of the numerous electron-dense vesicles derived from the Golgi complex forms this latter structure. Beneath the PAV, a short, straight cylinder corresponding to the acrosomal tube begins to develop (Figs 3A-F; 4A-C). This latter tube increases in length and finally borders upon the nucleus (Fig. 4C). Thereafter, it becomes longer and twisted, (Fig. 4B). In the final stages of acrosome morphogenesis and soon afterward, the acrosomal vesicle folds inside the tube (not shown). The lumen of this tube, which encompasses electron-dense granular material (subacrosomal material), will generate the axial rod (perforatorium) (Fig. 5A). The posterior portion of the axial rod terminates with a button-like structure called the 'basal knob' (Fig. 5A).

Nuclear elongation and condensation of the chromatin

The degree of chromatin condensation and the nuclear shape change continually during spermiogenesis. At first, in the early spermatids, the nucleus with large clumps of euchromatin is rounded (Figs 3A-C). Then, it assumes a finely granular aspect and an ovoidal shape (Fig. 3E). After that, the nucleus becomes longer and thinner, presenting a lamellar shape (Figs 3F-H; 4 C). The amount of heterochromatin increases gradually and progressively condenses to form straight cylinders (Figs 3F-I; 4C). Finally, the nucleus is a completely electron-dense and homogeneous corkscrewed structure (Figs 5B, C, H). Changes in the nuclear shape are accompanied by the presence of a microtubular manchette, which appeared in the early stages of spermiogenesis (Figs 3B-E). The microtubular manchette and the residual cytoplasm are eliminated before the late spermatids become spermatozoa (Figs 5A-H).

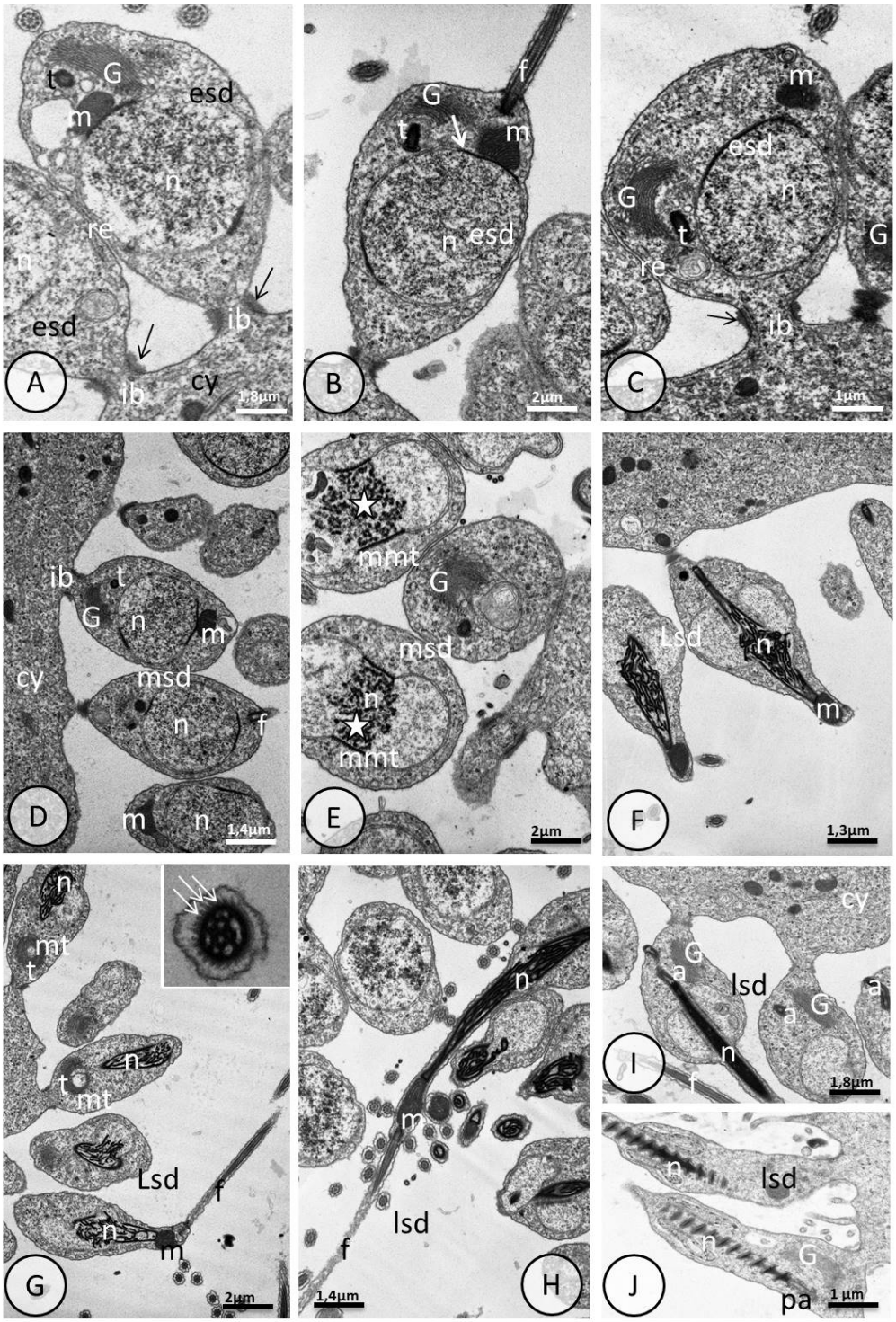

Fig. 3. A, B – Fragments of cysts uniting early spermatids (esd). Note that the Golgi complex (G) is in the apical pole of the spermatid. An acrosomal tube (t) is located near the Golgi complex. Note that the mitochondrion (m) migrates from the basal pole to the apical region. The distal centriole gives rise to the flagellum (f). The nuclei (n), endoplasmic reticulum (re), cytophore (cy), intercellular bridge (ib) and electron-dense rim of the intercellular bridges (black arrows) are visible. Note the electrodense material between the base of the nucleus and the mitochondrion (white arrow). TEM. C – Early to mid-spermatids. Note the Golgi complex (G) migration to the basal part of the cell, whereas the mitochondrion (m) occupies the apical pole. The nuclei (n), cytophore (cy) and intercellular bridge (ib) are visible. D – Part of a cyst with mid-spermatids (msd). Note the final distribution of the organelles: the Golgi complex (G) is now located in the cell's basal part, and the mitochondrion (m) is in the apical pole. The flagellum (f), acrosomal tube (t), nuclei (n), endoplasmic reticulum (re), cytophore (cy) and intercellular bridge (ib) are visible. E – Mid-spermatids (msd). Beginning of chromatin condensation (asterisks); also note the elongation of the nucleus (n). The manchette of microtubules (mmt) is visible. F-J – Late spermatids (lsd). F-H – The nucleus (n) becomes longer and thinner, showing a lamellar shape; the midpiece (m) reaches its final arrangement along the axoneme (f) in Figures G-H – Note the helical manchette of microtubules (mt) around the nucleus (n). *Inset*: Details of the manchette of microtubules (arrows). I – The nucleus (n) is a straight electron-dense cylinder. Twisted acrosome (a), Golgi complex (G), flagellum (f) and cytophore (cy) are visible. J – The nucleus (n) becomes a homogeneous corkscrew-shaped structure at this advanced stage. A part of the posterior acrosome (pa) near the Golgi complex (G) is visible. TEM.

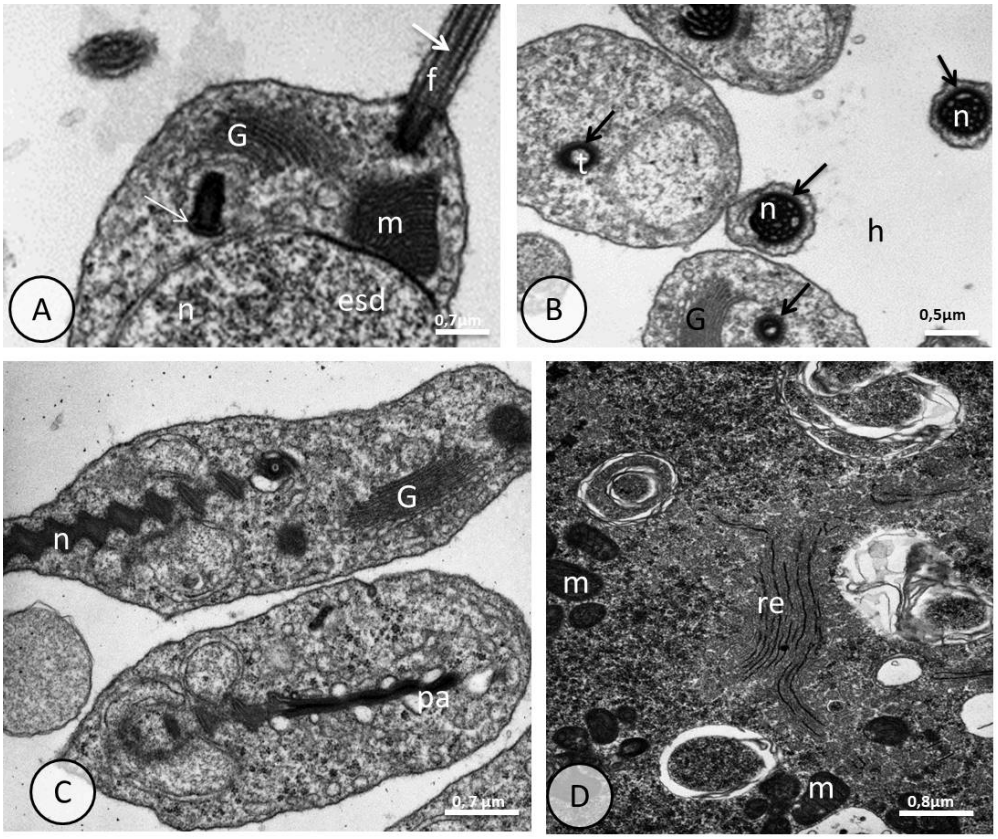

Fig. 4. Acrosome morphogenesis. A – Early spermatid (esd). Note the PAV near the Golgi complex (G). The flagellum (f) is of a prominent, electron-dense central sheath type (arrow). Mitochondrion (m) and nucleus (n) are visible. B – Mid-spermatids. The helical manchette is comprised of microtubules (arrows) around the acrosomal tube (t) and around the nuclei (n). The Golgi apparatus (G) and the nuclei (n) inside hemocoel (h) are visible. C – Note the acrosomal tube (t) and posterior acrosome (pa). The Golgi apparatus (G) and the nuclei (n) are visible. D – A portion of the cytophore interconnecting late spermatids. Note the endoplasmic reticulum (re) and mitochondria (m) accumulation. TEM.

D i f f e r e n t i a t i o n o f t h e m i d d l e p i e c e

In the early stage of development (spermatocytes/early spermatids), several mitochondria occupy the basal cell pole (not shown). All the mitochondria, except the large one that occupies the middle piece, have disappeared in subsequent stages. The persistent mitochondrion assumes a cup-like shape (Fig. 3A-D). It adheres closely to the base of the nucleus, but it is separated from the nucleus by electron-dense material (Fig. 3A, D). As spermiogenesis progresses, the microtubules forming the manchette start growing (Fig. 3E). The manchette is incomplete at first (Fig. 3E). During later developmental stages, the mitochondrion begins to elongate, thus reducing its diameter (Figs 3F, H). It gradually assumes a cylindrical shape (Figs 5G, H) and is eventually encompassed by a thin layer of dense material that forms the mitochondrial sheath (Fig. 5D).

F l a g e l l u m m o r p h o g e n e s i s

In the early spermatids, an axoneme emerges from a centriole located on the apical pole, i.e. opposite to the intercellular bridge (Figs 3A-B). During spermiogenesis, glycogen granules accumulate next to the axonemal doublet (Fig. 4A). Two central microtubules of the axoneme are housed within a prominent, electron-dense central sheath (Figs 5D, E).

Mature spermatozoa

The following description refers to the mature sperm observed in the epididymis (Figs 1E, 6). The spermatozoon of *H. japonica* is filiform and possesses all the classic hirudinid features. It is built, in order, by an acrosome divided into an anterior and a posterior portion, an elongated, helicoidally arranged nucleus, a straight single mitochondrial midpiece surrounded by a sheath of electron-dense material, and a flagellum of the prominent central sheath type with an endpiece.

A c r o s o m e

The acrosome of the studied species consists of two portions: an anterior acrosome, which has the form of a corkscrew-like structure prolonging an acrosome or ‘acrosome proper’, also called the ‘posterior acrosome’ in hirudinids (for a review, see

Wissocq and Malécha, 1975 and Ben Ahmed *et al.* 2015a), and a posterior acrosome. The anterior electron-dense acrosome is ~3.1 µm ± 0.05 long (n = 2)) and consists of two helically arranged fibres, whose diameter decreases progressively towards the tip (Fig. 5A). The posterior acrosome is a straight crystalline tube ~0.81 ± 0.01 µm long (n = 2) (Figs 5A, B). This latter feature has a regular periodic structure surrounded by a helical ridge, and it encircles the acrosome rod (also called the 'perforatorium' by

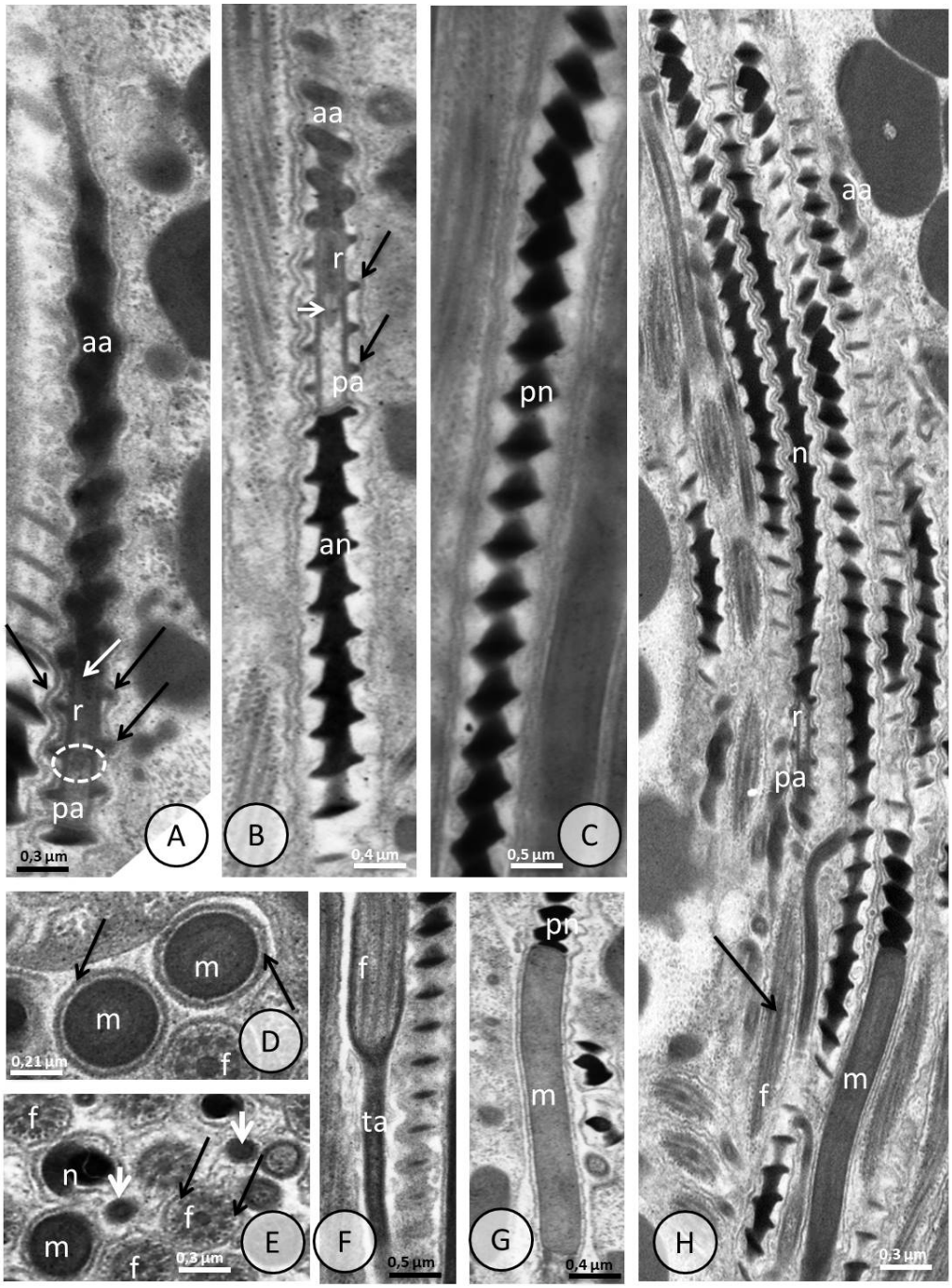

Fig. 5. Ultrastructure of the spermatozoa of *H. japonica* observed in epididymis. A – Longitudinal section showing the anterior acrosome (aa) and a portion of the posterior acrosome (pa). The acrosomal vesicle (white arrow), acrosome rod (r) and the rod ampoule (encircled) can be distinguished. Black arrows point to the helical ridge. B – Transitional zone between the posterior acrosome (pa) and a corkscrew-shaped anterior portion of the nucleus (an). The axial rod (r) can be seen with its 'rod ampoule' (white arrow) at the proximal extremity. A portion of the anterior acrosome (aa) and helical ridge (black arrows) are visible. C – A twisted column-shaped posterior portion of the nucleus (pn). D – Transverse section through the mitochondrion (m). Note the thin layer of electron-dense material (black arrow) surrounding the mitochondrion (m). Axoneme (f) are visible. E – Cross-sections through axonemes (f) and endpieces (short white arrows); nucleus (n); mitochondrion (m) glycogen granules (long black arrows). F – Transitional zone between axoneme (f) and the endpiece, also called the 'tapering appendage' (ta). G – Longitudinal section through the mitochondrion (m). A part of the posterior nucleus (pn) is also visible. H – A longitudinally-sectioned spermatozoon. The nucleus (n) is apically corkscrew-shaped and basally twisted column-shaped. The mitochondrion (m), anterior acrosome (aa), axial rod (r) and posterior acrosome (pa) are visible. Note that the axoneme (f) has a prominent central sheath (arrow).

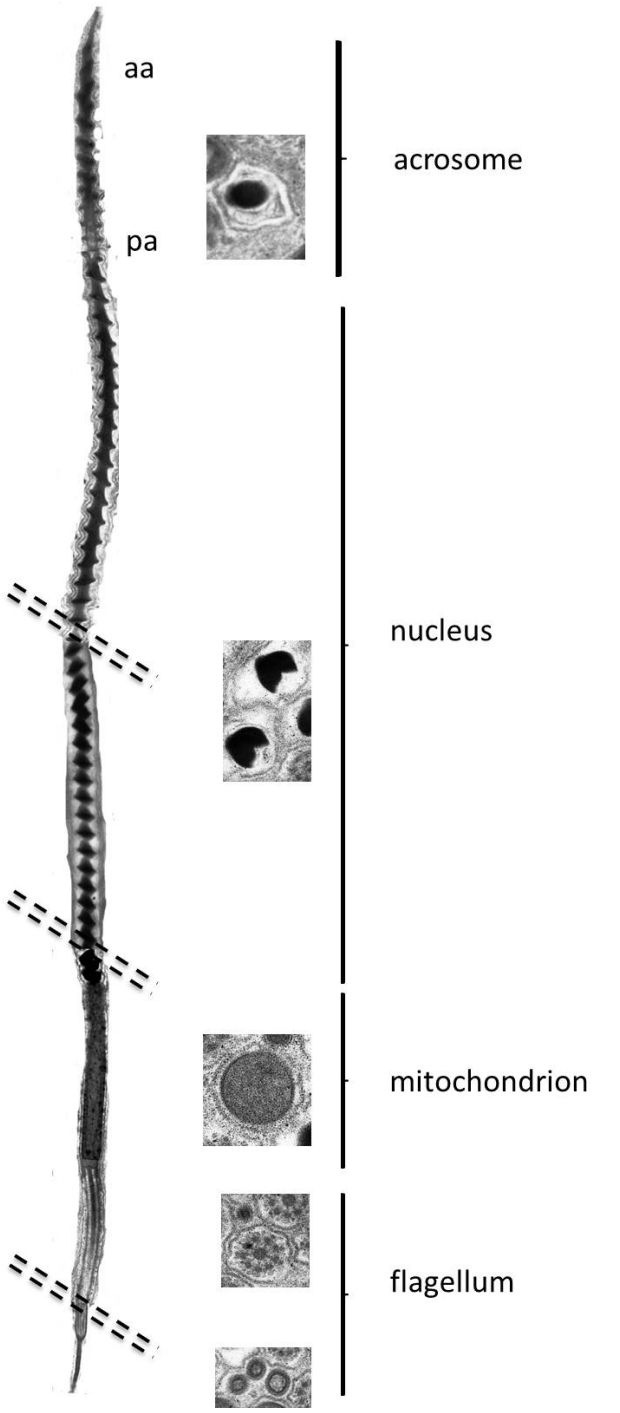

Fig. 6. Reconstruction of the ultrastructure of a mature sperm cell of *H. japonica* in longitudinal and cross-sections at various levels: aa: anterior acrosome, pa: posterior acrosome; additionally, nucleus, mitochondrion and flagellum are depicted.

Wissocq and Malécha, 1975) and the short vesicle (Fig. 5B, H). The acrosome rod and vesicles partially occupy the tube; thus, a hollow space that outlines the basal chamber is present between the vesicle and the base of the acrosome (Fig. 5B). The vesicle is invaginated basally to host the acrosome rod (Fig. 5B), which has a spherical structure in its proximal portion representing a 'rod ampoule' (Figs 5A, B, H). The acrosome rod protruding from the distal margin of the acrosomal tube terminates apically within the invagination of the acrosome vesicle (Figs 5B, H).

Nucleus

The nucleus is long (a length of up to 5.06 µm was measured) and has a filiform structure composed of completely condensed chromatin, the profile of which gradually changes from the tip to the base. Apically, it is corkscrew-shaped; whereas basally, it has a twisted-column shape (Figs 5B, C, H).

Midpiece

A single straight mitochondrion forms the midpiece (Figs 5G, H). It is ~2.4 ± 0.03 µm long (n = 3). At its proximal portion, the mitochondrion has a slight conical evagination protruding into the nucleus (Figs 5D, G, H). The mitochondrion is completely encompassed by a thin layer of an electron-dense substance (Figs 5D, E).

Flagellum

The tail is composed of an axoneme and an endpiece. The axoneme has the conventional 9 × 2 + 2 pattern of microtubule distribution (Fig. 5 E). Glycogen granules occur externally to the axonemal doublets (Fig. 5E). The flagellum of the mature spermatozoa is of the prominent central sheath type (PCs), according to Ferraguti (1984) (Figs 5 E, H). It ends in a narrow, specific, non-structured endpiece called a'tapering appendage' (Figs 5E, F). The length of this latter structure in the examined species was 1.6 µm.

Discussion

Clitellate characteristics of *H. japonica* spermatozoa

Our ultrastructural investigations revealed that the long and filiform spermatozoa of *H. japonica* are similar to the spermatozoa of other Clitellata adapted to internal fertilisation, and thus are classified as 'introsperm' (*sensu* Rouse& Jamieson 1987). Such spermatozoa also belong to the group described as 'modified' spermatozoa (*sensu* Franzén 1977). Moreover, the studied land leech spermatozoa showed a typical clitellate annelid ultrastructure. They have an acrosome tube with an acrosome rod, mitochondria between the nucleus and flagellum, and a central sheath in the flagellum. Generally, three main autapomorphic characters determine a clitellate spermatozoon: (1) the acrosome tube with a rod; followed by (2) the midpiece with one (Hirudinida and *Acanthobdella*) or many mitochondria (Branchiobdellida and Oligochaeta) interposed between

the nucleus and flagellum; and finally by (3) the 'prominent central sheath' in the flagellum (Ferraguti & Gelder 1991; Ferraguti & Erséus 1999; Ben Ahmed *et al.* 2015a). Within clitellates (Table 2), sperm typical for Oligochaeta *sensu stricto* (non-leech-like Clitellata) have a basal cylinder and tetragon fibres in the flagellum (Jamieson 1978; Ferraguti and Gelder 1991; Ben Ahmed *et al.* 2015a). Other features, such as coiled Golgi complexes (during spermiogenesis) and a flagellar tapering appendage filled with dense material, together with the absence of the tetragon fibres and a basal cylinder, are typical for the sperm in Hirudinida, Branchiobdellida and Acanthobdellida (Marotta *et al.* 2008; Ben Ahmed *et al.* 2015a). The sperm of Branchiobdellida are distinguished by a marginal helical fibre coiled throughout the flagellum (Ferraguti & Gelder 1991; Ben Ahmed *et al.* 2015a). The spermatozoa of *Acanthobdella peledina*, which was examined by Franzén (1991) and Westheide & Purschke (1996), resemble those of leeches in diverse aspects, i.e. a nuclear morphology (twisted or corkscrew only) and a single midpiece that is encompassed by an electron-dense sheath. However, the spermatozoa typical for Hirudinida exhibit two autapomorphic features: an anterior acrosome (Ferraguti & Gelder 1991; Ben Ahmed *et al.* 2015a) and a rod ampoule (Ben Ahmed *et al.* 2015a). Other typical features of hirudinean sperm, shared with all clitellates, seem to be a crystalline acrosome tube and a regular row of glycogen granules positioned externally to the axoneme (Ferraguti & Erséus 1999). This latter characteristic, together with the general slender morphology and the existence of an actin perforatorium, was considered by Ferraguti & Erséus (1999) to be of poor phylogenetic value; they suggested that these features may have appeared independently many times in different evolutionary lineages. It is believed that spermatogenesis and the sperm ultrastructure are especially helpful for a phylogenetic assessment within Clitellata; particularly in resolving the relationships between Acanthobdellida and Hirudinida (e.g. Erseus & Ferraguti 1995; Ferraguti & Erseus 1999; Ferraguti *et al.* 1999; Marotta *et al.* 2003, 2008; Cardini & Ferraguti 2004). Such autapomorphies as a twisted or corkscrew-shaped nucleus and a midpiece with a single mitochondrion encompassed by an electron-dense sheath support the grouping of *Acanthobdella peledina* (Acanthobdellida) as a sister to Hirudinida (for a review, see Ben Ahmed *et al.* 2015a). On the other hand, the secondary lack of the tetragonal fibres and basal cylinder (*sensu* Ferraguti 1984) in the mature sperm, as well as the presence of coiled Golgi vesicles during spermiogenesis and a flagellum tapering appendage are instead autapomorphies for the Branchiobdellida + Acanthobdellida + Hirudinida

Table 2

Comparison of ultrastructural characters of clitellate spermatozoa

Character	Clitellata			
	Oligochaeta (non leech-like oligochaetous Clitellata)	Hirudinea		
		Branchiobdellida	Acanthobdellida	Hirudinida
Anterior acrosome	Absent	Absent	Absent	Present
Acrosome tube	Present	Present	Present	Present
Acrosome rod (perforatorum)	Present	Present	Present	Present
Coiled Golgi vesicles during spermiogenesis	No	Yes	Yes	Yes
Corkscrew-shaped or twisted nucleus only	No	No	Yes	Yes
Mitochondrion between nucleus and flagellum	Yes	Yes	Yes	Yes
single mitochondrion	No	No	Yes	Yes
Dense material around mitochondria	No	No	Yes	Yes
Loss of basal cylinder	No	Yes	Yes	Yes
Prominent central sheath surround the flagellum	Present	Present	Present	Present
Loss of tetragon fibers in the flagellum of mature sperm	Yes	No	No	No
Dense sheath surrounding the flagellum	Absent	Absent	Present	Absent
Accessory fibers of the axoneme	Absent	Absent	Present	Absent
Helical marginal fiber around flagellum	Absent	Present	Absent	Absent
Terminal piece of the flagellum	Absent	Present	Present	Present

group (Marotta *et al.* 2008; Ben Ahmed *et al.* 2015a). Although the sister-group relationship between Acanthobdellida and Hirudinida is not in line with several previous molecular phylogenetic studies (Apakupakul *et al.* 1999; Erséus & Källersjö 2004; Gelder & Siddall 2001; Siddall *et al.* 2001; Siddall & Burreson 1998), some recent molecular analyses strongly support the sister relationship between these two taxa (Tessler *et al.* 2018; Philips *et al.* 2019). It is worth adding that numerous molecular analyses of the phylogenetic relationships among Clitellata have been based upon *A. peledina* contaminated by host DNA. Consequently, the obtained results were burdened with errors (Tessler *et al.* 2018; Philips *et al.* 2019).

Hirudinida characters of *H. japonica* spermatozoa

The *Haemadipsa japonica* sperm's organisation and ultrastructure resemble those of other studied hirudinids. These similarities between the spermatozoa may be regarded as features typical for Hirudinida, thus confirming the group's constancy as suggested by previous studies (Malécha 1975; Sawyer 1986; Bonet & Molinas 1988; Ben Ahmed *et al.* 2015a, b). Moreover, the sperm of the hirudinids is unquestionably the most complex spermatozoa within clitellates.

The corkscrew-shaped anterior acrosome, which is followed by the acrosome (called the 'posterior acrosome' in hirudinids, Wissocq & Malécha 1975), is incontestably unique (autapomorphic) for Hirudinida. The length of the anterior acrosome ('apex acrosomique' according to Wissocq & Malécha 1975) varies among leeches, e.g. 1.1 µm in *Hemiclepsis marginata* and 4 µm in *Piscicola geometra* (Wissocq & Malécha 1975). In *H. zeylanica,* the anterior acrosome measures 2.17 µm long (Ben Ahmed *et al.* 2015a), while in *H. japonica* it is slightly longer at 3.1 µm. Similarly, the posterior acrosome length is variable and reaches 1.5 µm in *H. zeylanica* (Ben Ahmed *et al.* 2015a) and 3.6 µm in *Branchellion torpedinis* (Wissocq & Malécha 1975). In the studied species, the posterior acrosome was shorter and measured only 0.81 µm long. In addition, the acrosome tube was pronounced and homogeneous in shape over its entire length. It appears that this latter structure is typically straight, crystalline and encompassed by a helical ridge, whose profile was variable among the studied species. This finding conforms with those for other species such as *Batracobdella paludosa* (Arcidiacono 1979), *H. zeylanica* and *Theromyzon tessulatum* (Ben Ahmed *et al.* 2015b); whereas *Batracobdella algira* (Ben Ahmed *et al.* 2019) showed a helical ridge with a changing morphology. It is well-developed distally toward the anterior acrosome but decreases in size proximally toward the nucleus. In contrast, in the case of *Placobdella costata*, the helical ridge is well-developed proximally toward the nucleus and distally toward the anterior acrosome, whereas it decreases in size in the central portion of the acrosome (Ben Ahmed *et al.* 2015b). The tube is inserted into the vesicle and the acrosome rod (perforatorium). In *H. japonica*, these two structures are only partially enclosed in the tube, thus defining a hollow space that separates the vesicle from the base of the acrosome, forming the 'basal chamber' as described by Ben Ahmed *et al.* (2015a) for *H. zeylanica*. Such a basal chamber has not been observed in *T. tessulatum*, *P. costata* (Ben Ahmed *et al.* 2015a), *B. algira* (Ben Ahmed *et al.* 2019), *Erpobdella octoculata*, *Hirudo medicinalis* or *Branchellion torpedinis* (Wissocq & Malécha 1975). However, it is clearly visible, but not described in *Hirudo troctina* (Ben Ahmed *et al.* 2015b) and *Dina lineata* (Bonet & Molinas 1988). Among Clitellata, this structure has been described in *A. peledina* by Marrota and Ferraguti (2009). In addition, the acrosome rod expands at its ends, forming a spherical structure, the so-called 'rod ampoule'. This latter structure was considered by Ben Ahmed *et al.* (2015a) as the second autapomorphic characteristic that defines a hirudinid spermatozoon, together with the anterior acrosome.

Similarly to all the hirudinids that have been studied, the nuclei of *H. japonica* spermatozoa show a helical structure. The nucleus consists of two parts, whose profiles gradually change from the tip to the base: an apical corkscrew-shaped section; and a basal twisted, column-shaped section. This finding is similar to the described nucleus from Hirudiniformes spermatozoa: *H. zeylanica*, *H. troctina* and *H. medicinalis* (Ben Ahmed *et al.* 2015a, 2015b; Garavaglia *et al.* 1974; Wissocq & Malécha 1975). As in Hirudiniformes, the nucleus in Erpobdelliformes has two distinguishable parts, which are determined by the nature of the helical thickenings (Garavaglia *et al.* 1974; Wissocq & Malécha 1975; Bonet & Molinas 1988). The nucleus of the spermatozoa in Glossiphoniformes and Piscicolidae, on the other hand, has a uniform appearance along its length (Ben Ahmed *et al.* 2019; Arcidiacono 1979; Ben Ahmed *et al.* 2015b; Damas 1968; Wissocq & Malécha 1975).

A single elongated mitochondrion, inserted between the nucleus and flagellum and encompassed by an electron-dense sheath, was found in the midpiece of the studied species. As in many hirudinids, the mitochondrion of *H. japonica* is straight. Among

the arhynchobdellids studied to date (i.e. *Hirudo medicinalis*, *H. troctina*, *Haemopis sanguisuga*, *H. zeylanica*, *Dina lineata*, *Erpobdella testacea*, *Erpobdella octoculata* and *Barbronia weberi*), only this latter salifid leech possesses a helical mitochondrion (Wissocq & Malécha 1975; Bonet & Molinas 1988; Ben Ahmed *et al.* 2015a; Gouda 2013). Moreover, the length of the midpiece is variable among leeches, with the shortest one before this study measured in *H. zeylanica* and *B. algira*, being 3 µm long (Ben Ahmed *et al.* 2015b; 2019). In the studied species, the mitochondrion is shorter and has a length of just 2.4 µm. The tail of *H. japonica* is composed of an axonemic region and an endpiece. The axonemic portion of the tail is of the characteristic prominent central sheath type (PCS), with nine external doublets. The length of the endpiece is variable among leeches. It ranges from 1.6 µm in *H. troctina* (Ben Ahmed *et al.* 2015b) and in *H. japonica* (present study) to 40 µm in *E. testacea* (Wissocq & Malécha 1975). A length up to 0.68 µm was measured in the congenerous species *H. zeylanica* (Ben Ahmed *et al.* 2015b).

To summarise, the spermatozoon of *H. japonica* has all the typical hirudinid features: an acrosome divided into an anterior and a posterior portion, a helicoidally arranged nucleus, a single mitochondrion surrounded by a sheath of electron-dense material, and a flagellum of the prominent central sheath type with an endpiece.

Hirudiniformes characteristics of *H. japonica* spermatozoa

Compared with all the already examined Hirudiniformes – *H. zeylanica* (Ben Ahmed *et al.* 2015a), *H. sanguisuga* (Wissocq & Malécha 1975), *H. troctina* (Ben Ahmed *et al.* 2015b) and *H. medicinalis* (Wissocq & Malécha 1975; Garavaglia *et al.* 1974) – the spermatozoa of *H. japonica* share many common features with them, thus confirming the close phylogenetic relationships within this taxon. In fact, from these studies and those for the analysed leeches above, we may present the following general characteristics of the hirudiniform spermatozoon: a filiform shape; a helical short anterior acrosome followed by a posterior acrosome; a helicoidal nucleus with two regions and two fibres; one straight mitochondrion between the nucleus and flagellum; and a tail containing a 9 + 2 axoneme and an endpiece. The same ovary organisation among the hirudiniform leeches studied to date (Świątek & Urbisz 2019; Urbisz *et al.* 2020) and the same sperm ultrastructure strongly suggest the monophyly of Hirudiniformes, which was also indicated by a molecular analysis (Borda & Siddall 2004).

Comparison with *Haemadipsa zeylanica*

The morphology and the ultrastructure of the spermatozoa of *H. japonica* do not notably differ from the only land leech that has been examined at the ultrastructural level up to now: *H. zeylanica* (Ben Ahmed *et al.* 2015a). The spermatozoa of these two species possess all the typical hirudinid features. The anterior acrosome is composed of two fibres arranged in a helical manner. The thinnest one is twisted around the other fibre, which acts as the axis. The diameter of the anterior acrosome decreases progressively towards the tip, giving this region a corkscrew-shaped appearance. The posterior acrosome is surrounded by a helical ridge, with a crystalline tube that encloses the acrosome rod and the vesicle. This latter structure expands at its ends, forming the ‘rod ampoule’. It should be stressed here that the acrosome of both terrestrial species is similar, not only in the shape of the different components of the acrosome, but also in its size and the morphology of the helical ridge. Moreover, the profile of the nucleus of both species is identical and gradually changes from being apically corkscrew-shaped at the tip to a twisted column-shaped structure in the base. Concerning the midpiece, both species have a single straight mitochondrion encompassed by a sheath of electron-dense material. Likewise, the tail is composed of the characteristic prominent central sheath (PCS), and ends in a tapering appendage filled with homogeneous electron-dense material and lacking any axonemal structure.

On the other hand, the strong similarities between the spermatozoa within Hirudinida have been described previously in Hirudiniformes between the two medicinal leeches *H. troctina* and *H. medicinalis* (see Ben Ahmed *et al.* 2015b), as well as in Glossiphoniformes in the genus *Batracobdella* between *B. algira* (Ben Ahmed *et al.* 2019) and *B. paludosa* (Arcidiacono 1979). In fact, minor interspecific variations related to the length, diameter and spiralisation patterns of diverse cell regions have been noted in these leeches. These results confirm that, at least in the case of Hirudinida, the sperm cell has a poor phylogenetic value at the species level.

Acknowledgments

Part of this study was supported by the Japan Society for the Promotion of Science, KAKENHI [Grant Numbers JP17K20064 and JP18K14780]. We cordially thank the editor and reviewers, whose helpful and sincere comments have improved the manuscript.

Author Contributions

Research concept and design B.A.R., P.Ś.: Collection and/or assembly of data: B.A.R., P.Ś. R.K., J.P.; Data analysis and interpretation: B.A.R., P.Ś.; Writing the article: B.A.R.; Critical revision of the article: P.Ś., T.N.; Final approval of article: B.A.R., P.Ś.

Conflict of Interest

The authors declare no conflict of interest.

References

Apakupakul K., Siddall M.E., Burreson E.M. 1999. Higher-level relationships of leeches (Annelida: Clitellata: Euhirudinea) based on morphology and gene sequences. Mol. Phylogenet. Evol. **12**: 350-359. https://doi.org/10.1006/mpev.1999.0639

Arcidiacono G. 1979. Differentiation of the *Batracobdella paludosa* sperm cell. Acta. Embryol. Morphol. Exp. **2**: 209-228.

Ben Ahmed R., Bacchetta R., Boesi R., Froman N., Marotta R., Ferraguti M. 2015a. The spermatozoa of Hirudinea with examples from three different taxa. Zool. Anz. 255: 54-61. https://doi.org/10.1016/j.jcz.2015.02.001

Ben Ahmed R., Małota K., Jarosz N., Świątek P. 2019. Microscopic analysis of spermatogenesis and mature spermatozoa in the amphibian leech *Batracobdella algira* (Annelida, Clitellata, Hirudinida). Protoplasma. 256:1609-1627. https://doi.org/10.1007/s00709-019-01407-w

Ben Ahmed R., Tekaya S., Urbisz A.Z., Świątek P. 2015b. Ultrastructural study of spermatogenesis and sperm in the African medicinal leech *Hirudo troctina* Johnson, 1816 (Annelida, Hirudinida). Tissue Cell. **47**: 242-253. https://doi.org/10.1016/j.tice.2015.03.002

Bonet S., Molinas M. 1988. Ultrastructure of the sperm and spermatogenesis and spermiogenesis of *Dina lineata* (Hirudinea, Erpobdellidae). Gamete. Res. **19**:177-190. https://doi.org/10.1002/mrd.1120190208

Bonet S., Molinas M., Garcia-Mas I. 1988. Testicular spermatozoa and male germ cells evolution in *Dina lineata* (Hirudinea, Erpobdellidae) studied by scanning electron microscopy. Butll. Inst. Catalana d'Hist. Nat. **55**: 17-25. https://doi.org/10.1002/mrd.1120190208

Borda E., Siddall M. E. 2004. Arhynchobdellida (Annelida: Oligochaeta: Hirudinida): phylogenetic relationships and evolution. Mol. Phylogenet. Evol. **30**: 213-225. https://doi.org/10.1016/j.ympev.2003.09.002

Cardini A., Ferraguti M. 2004. The phylogeny of Branchiobdellida (Annelida, Clitellata) assessed by sperm characters. Zool. Anz. **243**: 37-46. https://doi.org/10.1016/j.jcz.2004.06.001

Damas D. 1968. Origine et structure du spermatophore de *Glossiphonia complanata* (L.) (Hirudinée, Rhynchobdelle). Arch. Zool. Exp. **109** : 79-85.

Erséus C., Ferraguti M. 1995. The use of spermatozoa ultrastructure in phylogenetic studies of Tubificidae (Oligochaeta). In: Jamieson, B.G.M., Ausio, J., Justine, J.L (ed). Advances in Spermatozoal Phylogeny and Taxonomy. Mém. Mus. Natn. Hist. Nat, pp. 189-201

Erséus C., Källersjö M. 2004. 18S rDNA phylogeny of Clitellata (Annelida). Zool. Scr. **33**: 187-196. https://doi.org/10.1111/j.1463-6409.2004.00146.x

Fahmy M., Ravelomanantsoa N.A.F., Youssef S., Hekkala E., Siddall M. 2019. Biological inventory of Ranomafana National Park tetrapods using leech-derived iDNA. Eur. J. Wildl. Res. **65**: 70. https://doi.org/10.1002/edn3.474

Ferraguti M. 1984. The comparative ultrastructure of sperm flagella central sheath in Clitellata reveals a new autapomorphy of the group. Zool. Scr. **13**: 201-207.

Ferraguti M., Erséus C. 1999. Sperm types and their use for a phylogenetic analysis of aquatic clitellates. Hydrobiologia. **402**: 225-237. https://doi.org/10.1023/A:1003752811830

Ferraguti M., Erséus C., Kaygorodova I., Martin P. et al. 1999. In: Healy, B.M. (ed.). New sperm types in Naididae and Lumbriculidae (Annelida: Oligochaeta) and their possible phylogenetic implications. Aquatic Oligochaetes: Proceedings of the 7th International Symposium on Aquatic Oligochaetes held in Presque Isle. Maine, USA, 18-22 August 1997. Dev. Hydrobiol. **139**: 213-222. https://doi.org/10.1139/z91-269

Ferraguti M., Gelder S.R. 1991. The comparative ultrastructure of spermatozoa from five branchiobdellidans (Annelida Clitellata). Can. J. Zool. **69**: 1945-1956. https://doi.org/10.1139/z91-269

Franzén Å. 1977. Gametgenesis of bryozoans. In: Woollacott, R.M., Zimmer, R.L. (ed.), Biology of Bryozoans. Academic Press, New York. Pp. 1-22.

Franzén Å. 1991. Spermiogenesis and sperm ultrastructure in *Acanthobdella peledina* (Hirudinea) with some phylogenetic considerations. Invertebr. Reprod. Dev. **19**:245-256. https://doi.org/10.1016/j.tice.2015.03.002

Garavaglia C., Lora Lamia Donin C., Lanzavecchia G. 1974. Ultrastructural morphology of spermatozoa of hirudinea. J. Submicr. Cytol. **6**: 229-244 https://doi.org/10.1016/j.tice.2015.03.002

Gelder S. R., Siddall M. E. 2001. Phylogenetic assessment of the Branchiobdellidae (Annelida, Clitellata) using 18S rDNA, mitochondrial cytochrome c oxidase subunit I and morphological characters. Zool. Scr. **30** : 215-222. https://doi.org/10.1046/j.1463-6409.2001.00063.x

Gouda H.A. 2013. Spermatogenesis, spermiogenesis and sperm transfer in two freshwater leeches from assiut. Egypt. Res. Zool. **3**: 45-55. https://doi.org/10.5923/j.zoology.20130302.01

Hanya G., Morishima K., Koide T., Otani Y., Hongo S., Honda T., Okamura H., Higo Y., Hattori M., Kondo Y., Kurihara Y., Jin S., Otake A., Shiroisihi I., Takakuwa T., Yamamoto H., Suzuki H., Kajimura H., Hayakawa T., Suzuki- Hashido N., Nakano T. 2019. Host selection of haematophagous leeches (*Haemadipsa japonica*): implications for iDNA studies. Ecol. Res. **34**: 842-855. https://doi.org/10.1111/1440-1703.12059

Jamieson B.G.M. 2006. Non-leech Clitellata. In: Rouse, G., Pleijel, F. (Eds.), Reproductive biology and phylogeny of Annelida, Enfield (NH). Science Publishers, Jersey, Plymouth. Pp. 235-392.

Jamieson B.G.M. 1978. A comparison of spermiogenesis and spermatozoal ultrastructure in megascolecid and lumbricid earthworms (Oligochaeta, Annelida). Aust. J. Zool. **26**: 225-240. https://doi.org/10.1071/ZO9780225

Lai Y.T., Nakano. T., Chen J.H. 2011. Three species of land leeches from Taiwan, *Haemadipsa rjukjuana* comb. n., a new record for *Haemadipsa picta* Moore, and an updated description of *Tritetrabdella taiwana* (Oka). ZooKeys. **139**: 1-22. https://doi.org/10.3897/zookeys.139.1711

Malécha J. 1975. Étude ultrastructurale de la spermiogénèse de *Piscicola geometra* (Hirudinée, Rhynchobdelle). J. Ultrastruct. Res. **51**: 188-203. https://doi.org/10.1016/S0022-5320(75)80147-X

Marotta R., Ferraguti M. 2009. Sperm ultrastructure in assessing phylogenetic relationships among clitellate annelids. In: Shain DH (ed.) Annelids in Modern Biology. Wiley-Blackwell, Hoboken, NJ. Pp. 314-327. https://doi.org/10.1046/j.1463-6409.2002.00117.x

Marotta R., Ferraguti M., Erséus C. 2003. A phylogenetic analysis of Tubificinae and Limnodriloidinae (Annelida Clitellata, Tubificidae) using sperm and somatic characters. Zool. Scr. **32**: 255-278 . https://doi.org/10.1046/j.1463-6409.2002.00117.x

Marotta R., Ferraguti M., Erséus C., Gustavsson L.M. 2008. Combined data phylogenetics and character evolution of Clitellata (Annelida) using 18S rDNA and morphology. Zool. J. Linnean Soc. **154**: 1-26. https://doi.org/10.1111/j.1096-3642.2008.00408.x

Morishima K., Fukui E., Aizawa M. 2022. Concordant genetic structures of sika deer and Japanese land leeches suggest that the current range expansion of *Haemadipsa japonica* is dependent on sika deer migration: A case study from Tochigi Prefecture, Japan. Ecological research. **38** : 200-210. https://doi.org/10.1111/1440-1703.12366

Phillips A.J., Dornburg K., Zapfe L., Frank E., Anderson S., James W., Christer E., Emily M. L., Lemmon A. R., Williams B.W. 2019. Phylogenomic Analysis of a Putative Missing Link Sparks Reinterpretation of Leech Evolution. Genome Biol. Evol. **11**: 3082-3093. https://doi.org/10.1093/gbe/evz120.

Rouse G. W., Jamieson B. G. M. 1987. An ultrastructural study of the spermatozoa of the polychaetes *Eurythoe complanata* (Amphinomidae), *Clymenella* sp. and *Micromaldane* sp. (Maldanidae), with definition of sperm types in relation to reproductive biology. J. Submicrosc. Cytol. **19**: 573-584.

Sawyer R.T. 1986. Leech Biology and Behaviour. Clarendon Press, Oxford.

Schnell I.B., Sollmann R., Calvignac-Spencer S., Siddall M.E., Yu D.W., Wilting A., Gilbert M.T.P. 2015. iDNA from terrestrial haematophagous leeches as a wildlife surveying and monitoring tool – prospects, pitfalls and avenues to be developed. Frontiers Zool. **12**: 24. https://doi.org/10.1186/s12983-015-0115-z

Siddall M.E., Apakupakul K., Burreson E.M., Coates K.A., Erséus C., Gelder S.R., Källersjö M., Trapido-Rosenthal H. 2001. Validating Livanow: molecular data agree that leeches, Branchiobdellidans, and *Acanthobdella peledina* form a monophyletic group of Oligochaetes. Mol. Phylogenet. Evol. **21**: 346-351. https://doi.org/10.1006/mpev.2001.1021

Siddall M.E., Burreson E.M. 1998. Phylogeny of leeches (Hirudinea) based on mitochondrial cytochrome c oxidase subunit I. Mol. Phylogenet. Evol. **9** : 156-162 https://doi.org/10.1006/mpev.1997.0455

Sket B., Trontelj P. 2008. Global diversity of leeches (Hirudinea) in freshwater. Hydrobiologia. **595**: 129-137. https://doi.org/ 10.1007/s10750-007-9010-8

Świątek P., Urbisz A.Z. 2019. Architecture and Life History of Female Germ-Line Cysts in Clitellate Annelids. W. Tworzydło, Sz Bilinski (Eds.), Evo-Devo: Non-model Species in Cell and Developmental Biology. Results and Problems in Cell Differentiation, Springer, Cham, Switzerland. **68**: Pp. 515-551.

Tessler M.D., de Carle M.L., Voiklis O., Gresham A., Neumann J. S., Cios, S., Siddall M.E. 2018. Worms that suck: Phylogenetic analysis of Hirudinea solidifies the position of Acanthobdellida and necessitates the dissolution of Rhynchobdellida. Mol. Phylogenet. Evol. **127**: 129-134. https://doi.org/10.1016/j.ympev.2018.05.001

Urbisz A.Z., Nakano T., Świątek P. 2020. Ovary cord micromorphology in the blood-sucking haemadipsid leech *Haemadipsa japonica* (Hirudinida: Arhynchobdellida: Hirudiniformes). Micron. **138**: 102929. https://doi.org/10.1016/j.micron.2020.102929

Westheide W., Purschke G. 1996. Proacrosome and acrosome of the spermatozoon in *Acanthobdella peledina* (Annelida: Clitellata). Inv. Reprod. Dev. **29** : 223-230. https://doi.org/10.1080/07924259.1996.9672516

Wissocq J.C.L., Malécha J. 1975. Étude des spermatozoïdes d'hirudinées à l'aide de la technique de coloration negative. J. Ultrastruct. Res. **53**: 340-361. https://doi.org/10.1016/S0022-5320(75)80074-8